Biochimica et Biophysica Acta 1847 (2015) 505–513

Contents lists available at ScienceDirect

Biochimica et Biophysica Acta

journal homepage: www.elsevier.com/locate/bbabio

The *a* subunit of the A_1A_O ATP synthase of *Methanosarcina mazei* Gö1 contains two conserved arginine residues that are crucial for ATP synthesis

Carolin Gloger, Anna-Katharina Born, Martin Antosch [1], Volker Müller *

Molecular Microbiology & Bioenergetics, Institute of Molecular Biosciences, Johann Wolfgang Goethe Universität Frankfurt, Max-von-Laue-Str. 9, 60438 Frankfurt, Germany

ARTICLE INFO

Article history:
Received 20 October 2014
Received in revised form 24 January 2015
Accepted 17 February 2015
Available online 25 February 2015

Keywords:
Archaea
Energy conservation
Methanogens
Ion translocation
Site directed mutagenesis

ABSTRACT

Like the evolutionary related F_1F_O ATP synthases and V_1V_O ATPases, the A_1A_O ATP synthases from archaea are multisubunit, membrane-bound transport machines that couple ion flow to the synthesis of ATP. Although the subunit composition is known for at least two species, nothing is known so far with respect to the function of individual subunits or amino acid residues. To pave the road for a functional analysis of A_1A_O ATP synthases, we have cloned the entire operon from *Methanosarcina mazei* into an expression vector and produced the enzyme in *Escherichia coli*. Inverted membrane vesicles of the recombinants catalyzed ATP synthesis driven by NADH oxidation as well as artificial driving forces. $\Delta\tilde{\mu}_{H^+}$ as well as ΔpH were used as driving forces which is consistent with the inhibition of NADH-driven ATP synthesis by protonophores. Exchange of the conserved glutamate in subunit *c* led to a complete loss of ATP synthesis, proving that this residue is essential for H^+ translocation. Exchange of two conserved arginine residues in subunit *a* has different effects on ATP synthesis. The role of these residues in ion translocation is discussed.

1. Introduction

ATP synthases from archaea form a distinct class of ATP synthases/ATPases, the A_1A_O ATP synthases [1–5]. Like the evolutionary related F_1F_O ATP synthases found in bacteria, mitochondria and chloroplasts and the V_1V_O ATPases found in organelles of eukaryotes, the A_1A_O ATP synthases consist of two motors coupled by a central and peripheral stalk(s) [6–12] (Fig. 1). The membrane-bound A_O motor contains subunits *a* and *c*, the peripheral stalks are made by subunits E and H and the A_1 motor including the central stalk by subunits A, B, C, D, and F [11,13–16]. The membrane-bound motor is a rotational machine that is driven by inward flux of ions, driven by the electrical field across the membrane [17,18]. Rotational movement is transmitted to the central stalk by a coupling of subunits *c* and F, and rotation of the central stalk then drives conformational changes in A_1 that lead to ATP synthesis [3,19].

The general physiological function of A_1A_O ATP synthases is to synthesize ATP at the expense of an electrochemical ion gradient [3,21]. In this regard, they are like F_1F_O ATP synthases. In contrast, their subunit composition resembles those of V_1V_O ATPases and their evolutionary close relatedness is also reflected by sequence analyses of their major subunits [22]. Thus, the A_1A_O ATP synthases are chimeric proteins combining functional features of F_1F_O ATP synthases and structural features of V_1V_O ATPases [3,22].

Intact holoenzymes of A_1A_O ATP synthases have been purified only from *Methanocaldococcus jannaschii* and *Pyrococcus furiosus*, their structures have been determined by electron microscopy at 18 [23] and 23 Å resolution [11], respectively, and after heterologous production in *Escherichia coli* from *Methanobrevibacter ruminantium* [24]. In addition, the subunits of the A_1 part A, B, C, D, F, E and H have been produced in *E. coli*, crystallized and high-resolution structures have been obtained [25–30]. Structures of the *c* ring from an A_1A_O ATP synthase present in the bacterium *Enterococcus hirae* [31] and the soluble part of *a* from *Meiothermus ruber* have also been obtained [32]. Moreover, subcomplexes of the A_1 motor were produced in *E. coli* [15,33–35]. Despite the considerable increase in structural information, the molecular basis of A_1A_O ATP synthase function is largely unknown. This is mainly due to the fact that detailed structure-function relationships by mutagenesis studies could not be established due to the lack of a genetic system for *M. jannaschii* and *P. furiosus*. This may be changing since a naturally transformable mutant of *P. furiosus* was described recently [36]. However, the A_1A_O ATP synthases from hyperthermophiles proved to be disadvantageous for studying ATP synthesis *in vitro*, since a functional proteoliposome system could not be established due to the instability of liposomes at 80 °C [23]. To circumvent the problem, we have

Abbreviations: DES, diethylstilbestrol; DCCD, *N,N′*-dicyclohexylcarbodiimide; DDM, n-dodecyl-β-D-maltoside; DTE, dithioerythritol; IPTG, Isopropyl-β-D-1-thiogalactopyranoside; IMVs, inverted membrane vesicles; LILBID-MS, laser induced liquid beam ion desorption mass spectrometry; psiG, pounds per square inch (gauge)

* Corresponding author. Tel.: +49 69 79829507; fax: +49 69 79829306.
E-mail address: vmueller@bio.uni-frankfurt.de (V. Müller).
[1] Present address: Cell Biology & Plant Biochemistry, University of Regensburg, Universitätsstraße 31, 93053 Regensburg, Germany.

http://dx.doi.org/10.1016/j.bbabio.2015.02.015
0005-2728/

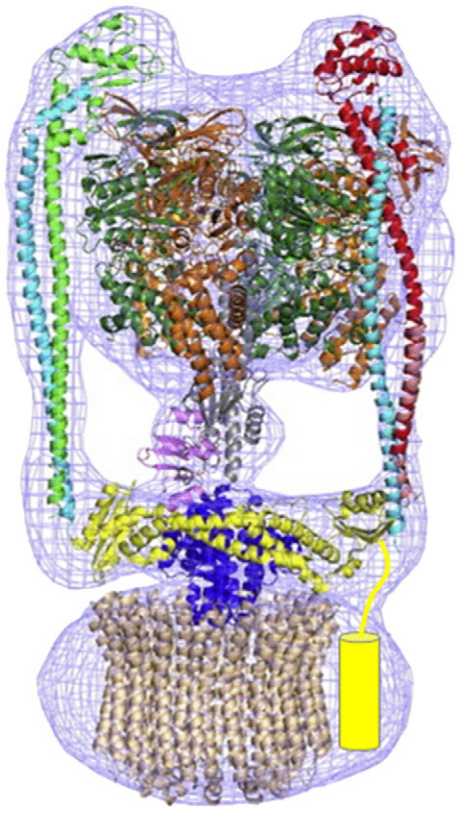

Fig. 1. 3D reconstruction map of the A_1A_O ATP synthase of *P. furiosus*. Structures of the single subunits were fitted into the individual densities of the EM map. Subunit A from *P. horikoshii* is shown in orange (PDB/3I4L), subunits B and F from *M. mazei* in dark green (PDB/2C61) and violet (PDB/2OV6), subunit C from *T. thermophilus* in blue (PDB/1R5Z), and subunit D and the *c* ring from *E. hirae* are colored in gray (PDB/3AON) and wheat (PDB/2BL2). The EH dimer from *T. thermophilus* is shown in green and cyan (PDB/3K5B); the E subunit from *P. horikoshii* and the H subunit from *T. thermophilus*, colored in red (PDB/4DT0) and cyan (PDB/3K5B), were fitted into the electron density of the second peripheral stalk. The soluble part of subunit *a* from *M. ruber* is shown in yellow (PDB/3RRK). The yellow barrel represents the membrane-embedded part of subunit *a*, for which no structure is available. Figure reproduced from [5,20].

expressed the *aha* operon encoding the A_1A_O ATP synthase from the mesophilic methanoarchaeon *Methanosarcina mazei* in *E. coli*. The A_1A_O ATP synthase was functionally produced in the F_1F_O ATP synthase-negative strain *E. coli* DK8 and we will present the first mutagenesis study on an A_1A_O ATP synthase that led to the identification of three residues important for ATP synthesis.

2. Materials and methods

2.1. Materials

All chemicals were obtained from AppliChem GmbH (Darmstadt), Carl Roth GmbH (Karlsruhe), Fluka Chemie GmbH (Buchs, Schweiz), ForMedium (Hunstanton, UK), Merck KG (Darmstadt), Serva Electrophoresis GmbH (Heidelberg) and Sigma-Aldrich Chemie GmbH (Steinheim). Restriction enzymes and DNA polymerase were from Fermentas GmbH (St. Leon-Rot) or New England Biolabs GmbH (Frankfurt) and Finnzymes (Vantaa, Finnland). Ni^{2+}NTA agarose was from Macherey and Nagel (Düren). The antibiotics ampicillin and chloramphenicol were obtained from Carl Roth GmbH (Karlsruhe) and Serva Electrophoresis GmbH (Heidelberg).

2.2. Organisms and plasmids

Methanosarcina mazei Gö1 (DSM 3647) was obtained from the 'Deutsche Sammlung für Mikroorganismen und Zellkulturen', Braunschweig, Germany, and grown under strictly anaerobic conditions as described [37,38]. *E. coli* DK8 (1100 Δ(*uncB-uncC*) ilv::Tn10) [39] and DH5α (*supE*44 Δ*lacU*169 Φ80*lacZ* ΔM15 *hsdr*17 *rec*A1 *end*A1 *gyr*A96 *thi*1 *rel*A1) [40] were obtained from the 'Deutsche Sammlung für Mikroorganismen und Zellkulturen', Braunschweig, Germany. The cells were grown in Luria-Bertani (LB) media at 37 °C; gene expression was induced at an $OD_{600\ nm}$ of 0.6–0.8 by addition of 1 mM IPTG. At an $OD_{600\ nm}$ of 1.5–1.7, the cells were harvested by centrifugation (11,300 *g*, 4 °C, 10 min) and stored at −80 °C. The plasmids used were pRPG54 [41], pRT1 [38], pSE420 (Invitrogen, Karlsruhe), pRIL (Stratagene, CA, USA), pA40, and pA40hisA.

2.3. Complementation assay

For complementation assays *E. coli* DK8 pA40, *E. coli* DK8 pRIL pA40 or *E. coli* DK8 pRPG54 (encoding the F_1F_O ATP synthase of *E. coli* under control of the native promoter) were grown on solid medium containing 33.8 mM KH_2PO_4, 48.7 mM K_2HPO_4, 19.7 mM NH_4SO_4, 146 μM $MgSO_4$, 0.5 μM $FeSO_4$, 10.2 μM $ZnCl_2$, 7.4 μM $CaCl_2$, 0.025% yeast extract, 50 μM thiamine, 0.2 mM isoleucine, 0.2 mM valine, pH 7 and 1.5% agar [42], over night at 37 °C. 1 mM IPTG and 10 mM glucose or 20 mM succinate were added to induce the production of the A_1A_O ATP synthase or as carbon source, respectively.

2.4. Construction of the plasmid pA40

The genes encoding the A_1A_O ATP synthase of *M. mazei* Gö1 are organized in the *aha* operon in the order 5′-*ahaH*, *ahaI*, *ahaK*, *ahaE*, *ahaC*, *ahaF*, *ahaA*, *ahaB*, *ahaD*, *ahaG*-3′. The whole operon and part of the *hypF* gene was cloned in one step using *Sal*I and *Sac*I from pRT1 [38] into the vector pSE420 resulting in the plasmid pA40, which includes the *aha* operon under the control of an IPTG inducible P_{trc} promoter. The identity of the construct was confirmed by restriction mapping and DNA sequence analyses.

2.5. Construction of the plasmid pA40hisA

To enable a one step purification of the A_1A_O ATP synthase a hexahistidine tag was genetically attached to the N-terminus of the A subunit using site directed mutagenesis. The following primers were used after phosphorylation to amplify the entire pA40 plasmid and insert six histidine codons at the 5′ end of *ahaA*: Mm*ahaA_his_SDM*$_{for}$ 5′-AGGTCAGTCGAGTGCACCAT CACCATCACCATGAAGTAAAAGGTGAAATT TATCGTG-3′ and Mm*ahaF_SDM*$_{rev}$ 5′-TTACTTCCACAGATCAACACCTAC-3′. The amplification product was digested with *Dpn*I, to break down template DNA, and afterwards religated resulting in the plasmid pA40hisA. The construct was verified by DNA sequence analyses.

2.6. Construction of the plasmids pA44, pA43, pA47, pA48, pA49*, pA50 and pA51

The following mutations were introduced *via* site directed mutagenesis with pA40hisA as template DNA and the following primers. *c*E65Q (pA44): Mm*ahaK***E65Q**for 5′-ATTCCA**C**AAACCATCGTTATCTTC-3′, Mm*ahaK***E65Q**SDM_rev 5′-GACAGTAAGAATAAGACCCTTAC-3′. *a*R563A (pA43): Mm*ahaI***R563A**for 5′CGTATGCT**GCT**ATTATCGCAGTC-3′, Mm*ahaI***R563A**SDM_rev 5′-AAAGTGCATTACCCATAAGAGATG-3′; *a*R563K (pA47): Mm*ahaI***R563K**forPhos 5′- CGTATGCT**AAG**ATTATCGC AGTCGGT-3′, Mm*ahaI***R563K**revPhos 5′-AAAGTGCATTACCCATAAGAGA TGG-3′; *a*R625A (pA48): Mm*ahaI***R625A**for 5′-**GC**GTTGCAGTATGTAG AATTCTTTGGAAAATTC-3′, Mm*ahaI***R625A**SDMrev 5′-GAGTGCGTGCAG TCCAGGAGCGATG-3′; *a*R625K (pA49*): Mm*ahaI***R625K**for 5′-**AAG**TTGCAGTATGTAGAATTCTTTGG AAAATTC-3′ with Mm*ahaI* **R625A**SDMrev. The double mutations were generated with pA48 (*a*R625A) or pA47 (*a*R563K) respectively as template DNA and the following primers: *a*R563A R625A (pA50): Mm*ahaI***R563A**for,

Mm*aha*I**R563A**SDM_rev; *a*R563K R625K (pA51): Mm*aha*I**R625A** SDMrev, Mm*aha*I**R625K**for. The mutations were introduced *via* the forward primers and are labeled in bold face. The plasmid constructs were verified by restriction mapping and sequence analyses.

2.7. Attempts to purify the A_1A_O ATP synthase via affinity chromatography

Two to three grams of cells (*E. coli* DK8 pRIL pA40hisA) were resuspended in 10 ml of TMGD buffer (50 mM Tris, 5 mM $MgCl_2$, 1 mM DTE, 0.1 mM phenylmethanesulfonyl fluoride and 10% (v/v) glycerol, pH 7.5). A spatula tip of DNAse was added and cells were disrupted by three passages through a French Press (1000 psiG). Cell debris was removed by centrifugation (23,700 *g*, 4 °C, 20 min), membranes were harvested by ultracentrifugation and washed in TMGD buffer once (160,000 *g*, 4 °C, 60 min). Washed membranes were resuspended in 1 ml TMGD buffer. The protein concentration was determined by Bradford [43] and adjusted to 10 mg/ml. The A_1A_O ATP synthase was solubilized from the membranes by addition of 1% (w/v) DDM and incubation for 60 min at 4 °C in motion. Residual membranes were removed by ultracentrifugation (160,000 *g*, 4 °C, 60 min), the supernatant containing the ATP synthase was incubated with 3 ml of Ni^{2+}NTA agarose for 60 min at 4 °C under shaking. Elution was performed after two washing steps with washing buffer (50 mM Tris/HCl, 300 mM NaCl, 20 mM imidazole, pH 8) with stepwise increasing concentrations of imidazole (110–190 mM) in 5 ml washing buffer. The ATP synthase containing fractions were collected, pooled and concentrated to a volume of 500 μl.

2.8. Preparation of inverted membrane vesicles

Three to six grams of *E. coli* cells were resuspended in 5 ml TMGD buffer (50 mM Tris, 5 mM $MgCl_2$, 1 mM DTE, 0.1 mM phenylmethanesulfonyl fluoride and 10% (v/v) glycerol, pH 7.5) per g cell material. Cells were disrupted by one passage through a French Press (400 psiG). Cell debris was removed by centrifugation (23,700 *g*, 4 °C, 20 min). The inverted membrane vesicles were harvested by ultracentrifugation and washed in TMGD-buffer once (160,000 *g*, 4 °C, 60 min). The protein concentration was determined as described [43]. The presence of the single subunits was verified by Western blot analyses as described [44]. To compare the amounts of ATP synthase in the membranes the blots were analyzed densitometrically *via* ImageJ (Wayne Rasband, USA).

2.9. NADH-driven ATP synthesis catalyzed by inverted membrane vesicles

The experiments were performed at 37 °C. 100 μg inverted membrane vesicles were diluted in 500–750 μl ATP synthesis buffer (25 mM Tris/HCl, 5 mM KH_2PO_4, 5 mM $MgCl_2$, 10% (v/v) glycerol, 5 mM NaCl, 0.12 mM ADP, pH 7.5) to a final protein concentration of 0.2 mg/ml. ATP synthesis was induced by the addition of 2 mM NADH from a stock solution. 5 μl samples were taken every minute and the ATP content was monitored using the luciferine–luciferase-assay as described [45]. In case of inhibitor studies, the vesicles were preincubated in the test buffer with the indicated inhibitor for 20 min at 37 °C. Inhibitors were added as ethanolic solutions, controls contained the solvent only.

2.10. Generation of artificial driving forces in inverted membrane vesicles of E. coli DK8 pRIL pA40

Different artificial driving forces were applied to inverted membrane vesicles to induce ATP synthesis. For $\Delta\tilde{\mu}_{H^+}$-induced ATP synthesis an artificial proton gradient as well as a potassium diffusion potential was applied to the membrane vesicles. Therefore, 7 μl of the inverted membrane vesicles (25–45 μg/μl) were diluted into 42 μl of reconstitution buffer (20 mM tricine, 20 mM succinate/NaOH, 0.6 mM KCl, 80 mM NaCl, 5 mM $MgCl_2$, 10% (v/v) glycerol, pH 8.0). 43 μl of this mixture were added to 217 μl of the acidic buffer (20 mM succinate/NaOH, 0.6 mM KCl, 2.5 mM $MgCl_2$, 5 mM NaH_2PO_4, 0.2 mM ADP, 1 μM valinomycin, pH 4.7) and preincubated for 2 min at 37 °C to decrease the internal and external pH to 5.2. By addition of the alkaline buffer (200 mM tricine/KOH, 50 mM KCl, 2.5 mM $MgCl_2$, 5 mM NaH_2PO_4, 0.2 mM ADP, pH 8.8) the external pH was increased to 8, whereby a proton gradient was established across the membrane. Due to the increase of the K^+ concentration and the presence of valinomycin an influx of K^+ into the vesicles was induced that generated an electric field ($\Delta\psi$) in addition. The final protein concentration was 0.4 mg/ml.

To apply an artificial proton gradient exclusively the previous protocol was modified: the K^+ concentration in both buffers was increased to 200 mM to avoid K^+ influx and the pH values of the alkaline buffer were varied to apply different proton gradients. The buffer compositions were the following for the acidic buffer (20 mM succinate, 200 mM KCl, 2.5 mM $MgCl_2$, 5 mM NaH_2PO_4, 0.2 mM ADP, 1 μM valinomycin, pH 4.7) and the alkaline buffer (200 mM tricine/KOH, 200 mM KCl, 2.5 mM $MgCl_2$, 5 mM NaH_2PO_4, 0.2 mM ADP, pH 4.7–9.3). For $\Delta\psi$-induced ATP synthesis the K^+ concentrations in the second buffer were varied, whereas the pH values were adjusted to 7.5. Therefore the vesicles were preincubated in buffer 1 (200 mM Tris/HCl, 0.6 mM KCl, 2.5 mM $MgCl_2$, 5 mM NaH_2PO_4, 0.2 mM ADP, 1 μM valinomycin, pH 7.5) and the reaction was started by the addition of the second buffer (200 mM Tris/HCl, 0.6–1147 mM KCl, 2.5 mM $MgCl_2$, 5 mM NaH_2PO_4, 0.2 mM ADP, pH 7.5).

3. Results

3.1. Production and cellular localization of the A_1A_O ATP synthase of M. mazei Gö1 in E. coli DK8 pRIL pA40

In previous studies the *aha* operon had been cloned into the plasmid pRT1 under the control of the arabinose-inducible P_{BAD} promoter [38]. To enable expression without the addition of the fermentable sugar arabinose the entire operon was recloned into pSE420, under the control of the IPTG-inducible P_{trc} promoter, resulting in the plasmid pA40. For purification of the enzyme a hexahistidine tag was introduced to the exposed N-terminal domain of the soluble subunit A [46]. Plasmid pA40 was transformed into the F_1F_O ATP synthase-negative strain *E. coli* DK8 [39]. To improve codon usage, the pRIL plasmid, coding for rare tRNAs, was transformed in addition. Transformants were grown on LB, gene expression was induced by addition of 1 mM IPTG and cells were harvested. Cell free extract was prepared and separated into cytoplasm and membrane fraction. Only in cells expressing the *aha* operon subunit A was detectable *via* Western blot analysis. It was present in the membrane fraction indicating that the methanoarchaeal ATP synthase was incorporated into the cytoplasmic membrane of *E. coli* (Fig. 2). Densitometric analysis revealed that membrane vesicles of *E. coli* DK8 pRIL pA40 contained 1.5 times more ATP synthase subunit A than vesicles of *E. coli* DK8 pA40. The presence of other subunits was also confirmed by Western blot analysis. Subunit *c* was found in the cytoplasmic membrane exclusively, whereas subunits D and F were also found in the cytoplasm. The A_1A_O ATP synthase produced in *E. coli* was capable of ΔpH-driven ATP-synthesis, as seen before with the enzyme produced from plasmid pRT1 (data not shown) [38].

3.2. The A_1A_O ATP synthase does not complement the ATPase deficient strain E. coli DK8

To establish a system that allows fast functional screening of various A_1A_O ATP synthase mutants, a complementation assay should be established. The F_1F_O ATP synthase-negative *E. coli* strain ought to be complemented by the produced A_1A_O ATP synthase to allow for growth on non-fermentable carbon sources such as succinate. Therefore, plasmid pA40 was transformed into *E. coli* DK8 pRIL and growth was analyzed on glucose or succinate as energy and carbon source. *E. coli* DK8

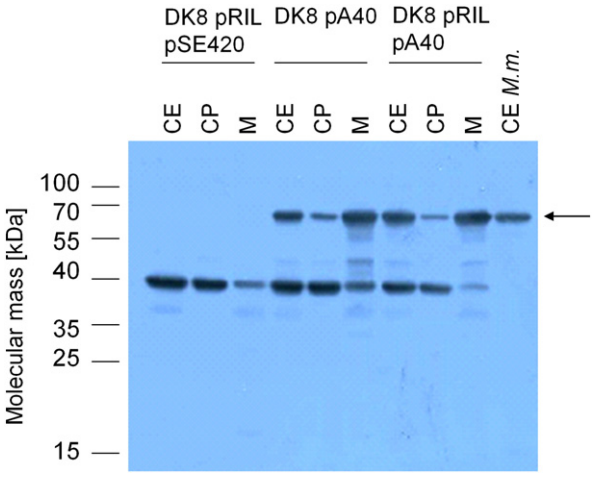

Fig. 2. Detection of subunit A in membrane vesicles of *E. coli* DK8 pRIL pA40. Cellular extract (CE), cytoplasm (CP) and membrane fractions (M), 2 μg each, of *E. coli* DK8 pRIL pSE420 (as negative control), DK8 pA40 and DK8 pRIL pA40 were prepared and analyzed by Western Blot with antibodies against AhaA. Cell extract from *M. mazei* (CE *M.m.*, 10 μg) was used as positive control. The presence of subunit A is marked.

pRPG54 (encoding the F_1F_O ATP synthase of *E. coli* under control of the native promoter) was used as positive control. The IPTG concentration, pH value and Na^+ concentration were varied, but the A_1A_O ATP synthase was not able to restore growth of *E. coli* DK8 pA40 on succinate, although *E. coli* DK8 pA40 and *E. coli* DK8 pRIL pA40 grew well on glucose. Since the complementation assay proved to be not feasible, we aimed to analyze ATP synthesis in a more defined *in vitro* system.

3.3. Attempts to purify the A_1A_O ATP synthase

To analyze the A_1A_O ATP synthase in an isolated system, we aimed to purify it from membranes of *E. coli* DK8 pRIL pA40hisA *via* affinity chromatography as described in Materials and methods section. First attempts appeared to be successful as a native complex of around 700 kDa was visible after native gel electrophoresis, but deeper analyses by analytical gel filtration revealed that the A_1A_O ATP synthase tends to disaggregate into subcomplexes during purification. To increase the stability of the whole enzyme during the purification process, we altered the conditions of growth and buffer composition, including different media, buffer components and stabilizing agents as compatible solutes, as well as the conditions for disruption of the cells, solubilization from the membranes with different detergents at temperatures from 4 °C to 37 °C and purification itself but with no significant effect. Since the purification was not successful, we analyzed the function of the ATP synthase in an inverted membrane vesicle system.

3.4. Inverted membrane vesicles of E. coli DK8 pRIL pA40 catalyze NADH-driven ATP synthesis

Inverted membrane vesicles (IMVs) were prepared from *E. coli* DK8. Upon the addition of NADH to the IMVs, it was oxidized with a rate of 32–48 nmol/min·mg protein. NADH oxidation was coupled to ATP synthesis in inverted membrane vesicles from *E. coli* DK8 pA40, *E. coli* DK8 pRIL pA40 and *E. coli* DK8 pRPG54 (Fig. 3A). IMVs from cells containing only the vector (*E. coli* DK8 pRIL pSE420) were not able to couple NADH oxidation to ATP synthesis. The presence of the pRIL plasmid during

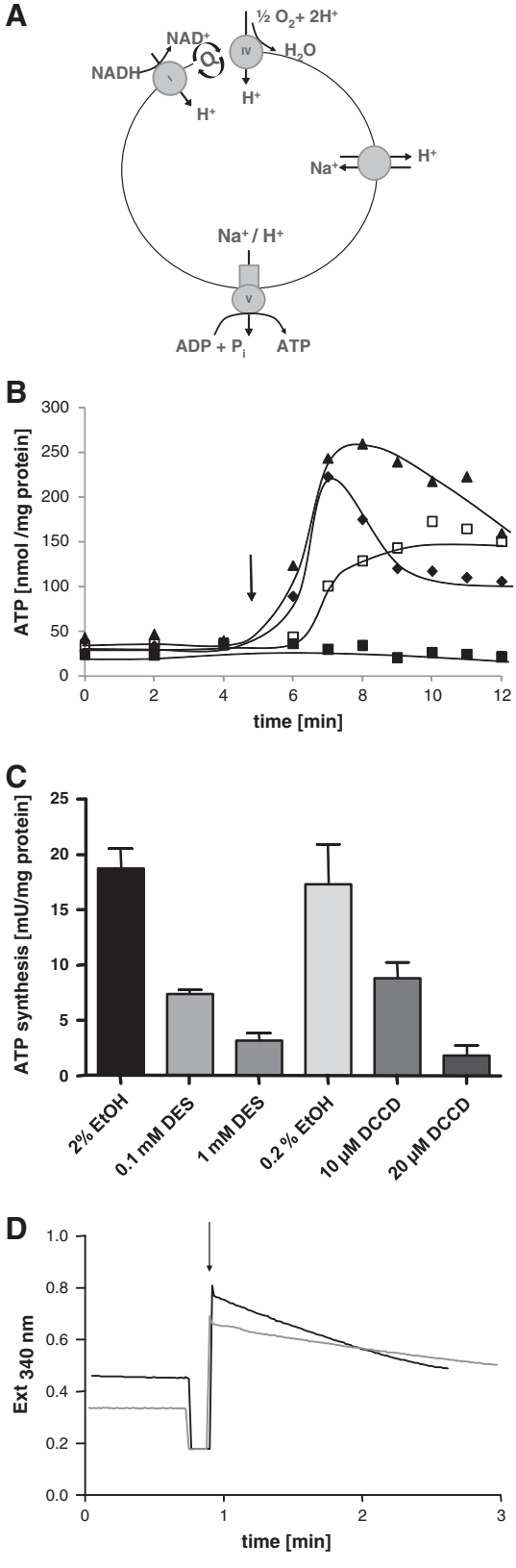

Fig. 3. ATP synthesis driven by oxidation of NADH catalyzed by inverted membrane vesicles of *E. coli* DK8. [A] Schematic model of inverted membrane vesicles energized by NADH oxidation. [B] Inverted vesicles of *E. coli* DK8 pA40 (□), DK8 pRIL pA40 (▲) as well as DK8 pRPG54 (♦) (encoding the F_1F_O ATPase of *E. coli*) and *E. coli* DK8 pRIL pSE420 (■) (negative control) were incubated in ATP synthesis buffer (25 mM Tris/HCl, 5 mM KH_2PO_4, 5 mM $MgCl_2$, 10% (v/v) glycerol, 5 mM NaCl, 0.12 mM ADP, pH 7.5; final protein concentration 0.2 mg/ml). At the time point indicated by the arrow, NADH was added to a final concentration of 2 mM and ATP was determined by the luciferine–luciferase-assay. [C] Preincubation of inverted membrane vesicles of *E. coli* DK8 pRIL pA40 in the presence of DCCD or DES inhibited ATP synthesis. Controls contained the solvent only. Shown is the average of two measurements. [D] NADH oxidation was followed at 340 nm (black). Preincubation in presence of 20 μM DCCD inhibited NADH oxidation (gray).

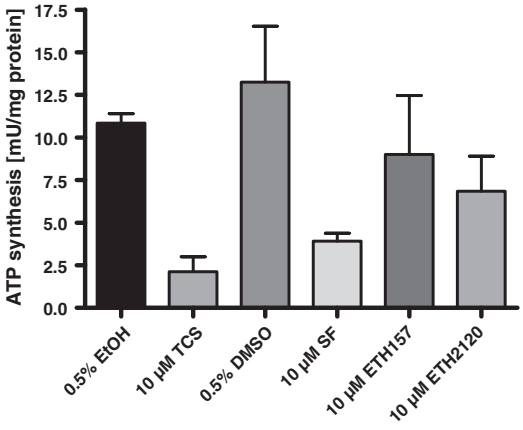

Fig. 4. NADH-driven ATP synthesis is inhibited by protonophores. 100 μg of inverted vesicles of *E. coli* DK8 pRIL pA40 were preincubated in ATP synthesis buffer for 20 min in presence of the ionophores indicated. ATP synthesis was started by the addition of NADH to a final concentration of 2 mM. ATP was determined by the luciferine–luciferase-assay. Controls contained the solvent only. Shown is the average of two measurements.

growth led to an increase in ATP synthesis activity (Fig. 3B). A ratio of 0.3 ATP per NADH was observed.

The NADH-driven ATP synthesis was inhibited by DCCD and DES, two known inhibitors for ATP synthases [47,48] (Fig. 3C). At the same time DCCD inhibited NADH oxidation by 65–86% (Fig. 3D), a clear evidence for a coupling of electron transfer and ATP synthesis. Protonophores like SF6847 and tetrachlorosalicylanilide (TCS) nearly abolished ATP synthesis, whereas the sodium ionophores ETH2120 and ETH157 had only a little effect (Fig. 4). ATP synthesis was independent from the Na^+ concentration, furthermore there was no protection from DCCD inhibition observed in the presence of 10 mM NaCl. Attempts to drive ATP synthesis by a ΔpNa or a ΔpNa in combination with a Δψ were not successful. ATP synthesis was also observed after oxidation of the alternative electron donors succinate and lactate. These experiments demonstrate that the A_1A_O ATP synthase is able to use the $\Delta\tilde{\mu}_{H^+}$ generated by NADH oxidation for ATP synthesis.

3.5. ATP synthesis driven by artificial driving forces in membrane vesicles of *E. coli* DK8 pRIL pA40

Next we analyzed whether ATP synthesis could be driven by an artificial $\Delta\tilde{\mu}_{H^+}$, made up by a pH gradient and a potassium diffusion potential or by a ΔpH or Δψ alone. Therefore, the IMVs were preincubated in an acidic buffer with low K^+ concentration, resulting in a low pH inside. After addition of the alkaline buffer containing high K^+ concentration and valinomycin, an artificial $\Delta\tilde{\mu}_{H^+}$ was established. An increase in ATP was observed after addition of the alkaline buffer (Fig. 5), and ATP was synthesized with activities of 19–25 mU/mg protein. Controls without ADP, IMVs or after addition of the acidic buffer instead of the alkaline buffer revealed that all compounds were essential for ATP synthesis. In the absence of valinomycin activities of 13–22 mU/mg protein were obtained.

To compare ΔpH and Δψ as driving forces for ATP synthesis, either the pH values or the K^+ concentrations of the two buffers were varied while the other conditions remained constant. With a ΔpH alone ATP synthesis was highest at a ΔpH of 3, which is equivalent to a membrane potential of −180 mV (Fig. 6). At a pH difference of 3.7 the ATP synthase activity decreased again. With a Δψ alone, no ATP synthesis was observed. These results demonstrate that a ΔpH alone is sufficient to drive ATP synthesis.

3.6. The conserved glutamate E65 within the c subunit of the A_1A_O ATP synthase of *M. mazei* is essential for ATP synthesis

Sequence alignments of the *c* subunit of *M. mazei* to those of other ATP synthases identified glutamate *c*E65 to the homologue of the "essential carboxylate" in F_1F_O ATP synthases and V_1V_O ATPases [49]. To analyze if this residue is essential for ATP synthesis and as a proof of principle experiment for the newly established mutagenesis system, *c*E65 was exchanged to glutamine (*c*E65Q) *via* site directed mutagenesis. To test the ability to synthesize ATP, IMVs of cells containing the ATP synthase variant (*E. coli* DK8 pRIL pA44) were prepared. Neither NADH oxidation nor an artificial $\Delta\tilde{\mu}_{H^+}$ drove ATP synthesis (data not shown). These results prove experimentally the role of *c*E65 in H^+ translocation in A_1A_O ATP synthases and demonstrate that the established mutagenesis system is suitable for the intended mutagenesis studies.

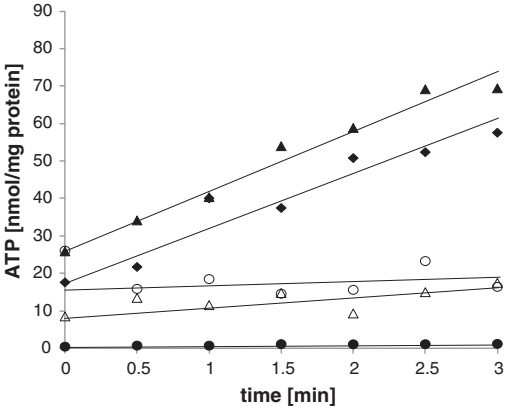

Fig. 5. $\Delta\tilde{\mu}_{H^+}$-driven ATP synthesis catalyzed by vesicles of *E. coli* DK8 pRIL pA40. Vesicles were preincubated in acidic buffer (20 mM succinate, 0.6 mM KCl, 2.5 mM $MgCl_2$, 5 mM NaH_2PO_4, 0.2 mM ADP, 1 μM valinomycin, pH 4.7) for 2 min at 37 °C. ATP synthesis was started by the addition of the alkaline buffer with high K^+ concentrations (200 mM tricine/KOH, 50 mM KCl, 2.5 mM $MgCl_2$, 5 mM NaH_2PO_4, 0.2 mM ADP, pH 8.8) (▲). One set contained no valinomycin (◆). Controls were performed either by addition of the acidic buffer instead of alkaline buffer (Δ) or contained no ADP (●) or no vesicles (○). The final protein concentration was 0.4 mg/ml.

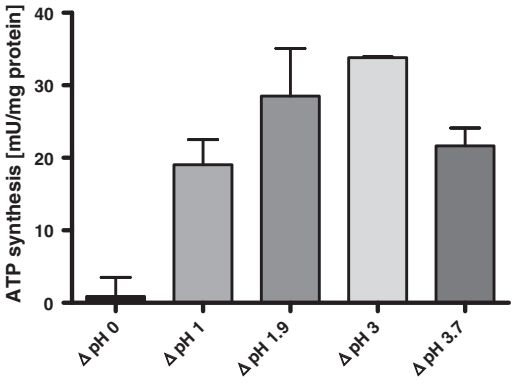

Fig. 6. ΔpH-driven ATP synthesis catalyzed by inverted membrane vesicles of *E. coli* pRIL pA40. The inverted membrane vesicles were preincubated in acidic buffer (20 mM succinate, 200 mM KCl, 2.5 mM $MgCl_2$, 5 mM NaH_2PO_4, 0.2 mM ADP, 1 μM valinomycin, pH 4.7) for 2 min at 37 °C. The reaction was started by addition of the alkaline buffer (200 mM tricine/KOH, 200 mM KCl, 2.5 mM $MgCl_2$, 5 mM NaH_2PO_4, 0.2 mM ADP, pH 4.7–9.3). The final protein concentration was 0.4 mg/ml. Shown is the average of two measurements.

```
S. cerevisiae    EEVGSGSHGEDFGDIMIHQVIHTIEFCLNCVSHTASYLRLWALSLAHAQLSSVLWTMTIQ 756
M. mazei         TYAGALILVIGVVMLTMGEGIKGPIELPSLMGNALSYARIIAVGLSSIYIAGTVNDIAFE 584
M. acetivorans   AYVGAVVLVLGIVMLTMGEGIKGPIELPSLMGNALSYARIIAVGLSSIYIASTVNDIAFE 583
M. barkeri       MYVGAVVLVLGIVMLAMGEGIAGIVELPSLMGNALSYARIIAVGLSSIYIASTVNDIAFG 573
M. maripaludis   IAVIVLCMIKGFMNGGILDALLGAMDITGFLGNVLSYARLLALCLATGGLAMAVN-IMAK 617

S. cerevisiae    IAFGFRGFVGVFMTVALFAMWFALTCAVLVLMEGTSAMLHSLRLHWVESMSKFFVGEGLP 816
M. mazei         MIWPDHSQIGAAAIAAIIVFILG--HGLNTILSIIAPGLHALRLQYVEFFGKFYEGGGRK 642
M. acetivorans   MIWADHSKIGFVAIAAILVFILG--HALNTVLSIIAPGLHALRLQYVEFFGKFYEGGGRK 641
M. barkeri       MVWPDHSKIGFAAIAAIIVFILG--HALNTVLSIIAPGLHALRLQYVEFFGKFYEGGGRK 631
M. maripaludis   LLGDAVPVIG--ILIAVVMLVFG--HSFNFVMNGLGSFIHSLRLHYVEFFGQYYEGGGKK 673
```

Fig. 7. Sequence alignment of *a* subunits of different methanoarchael ATP synthases to the *a* subunit of *S. cerevisiae*. The conserved residues are highlighted in gray, only parts of the sequences were aligned.

3.7. Two conserved arginine residues in the a subunit are crucial for ATP synthesis

The *a* subunits of F_1F_O have one and the *a* subunits of V_1V_O ATPases contain two conserved arginine residues that are crucial for ion translocation [50–52]. Sequence alignments of archaeal *a* subunits to other well characterized ATPases revealed that the first arginine residue is also conserved in A_1A_O ATP synthases. In addition, the second arginine which is conserved in subunit *a* from the V_1V_O ATPase of *Saccharomyces cerevisiae* is also conserved in the *a* subunit of *M. mazei* (Fig. 7).

To address their function in A_1A_O ATP synthases, the conserved arginine residues were deleted individually and in combination. Exchange of the first conserved arginine either to alanine (*a*R563A) or to lysine (*a*R563K) led to total loss of ATP synthesis activity (Fig. 8). When the second arginine was changed to alanine (*a*R625A) no ATP synthesis was observed as well. But when this arginine was changed to lysine (*a*R625K) almost 50% of the ATP synthesis activity was retained compared to the wild type. After the exchange of both arginines either to alanine (*a*R563A R625A) or to lysine (*a*R563K R625K) ATP synthesis was no longer observed (Fig. 8).

4. Discussion

A_1A_O ATP synthases have so far been purified only from hyperthermophilic archaea and their basic biochemical properties have been determined [10,11,13,14,23,53,54]. Molecular analyses on the role of individual subunits or amino acids have never been done due to the lack of a genetic system. The successful heterologous production of the ATP synthase from a mesophilic archaeon in a functional state in *E. coli* enabled us, for the first time, to perform a functional analysis on a molecular level. The ATP synthase from *M. mazei* produced in *E. coli* was active in ATP synthesis, as described before [38]. Unfortunately, the enzyme did not restore growth of *E. coli* DK8 on the non-fermentable carbon source succinate. This is most likely due to the ATP synthase activities of 25–50 mU/mg protein that are low but in the order of what is observed in IMVs of *M. mazei* (1–100 mU/mg; depending on the electron donor/acceptor used) [55–57]. However, the activities are orders of magnitudes lower than that of the enzyme from *E. coli* (0.46 U/mg protein–6 U/mg protein) [58,59]. These comparatively low activities may be due to the differences in codon usage between archaea and bacteria which could result in lower ATP synthase amounts synthesized. To circumvent this problem we added the pRIL plasmid coding for rare tRNAs. Both the higher amounts of ATP synthase detected in the membranes and the higher ATP synthase activities clearly showed an improvement. But nevertheless a complementation of *E. coli* DK8 could not be achieved. Although subunit A carried a hexahistidine tag and although it was apparently accessible to the Ni^{2+}-NTA-matrix, the enzyme could not be purified by affinity chromatography since it denatured on the column. Instability leading to the purification of only subcomplexes was observed very often [60–70]. This denaturation/inactivation was seen before with the enzyme directly enriched from cells of *M. mazei* [71]. Attempts to improve stability by using different detergents, buffers and purification protocols have been unsuccessful over decades till now. The hope to circumvent the problem using a one step purification proved delusory.

To compare the function of the variants to the wild type enzyme we analyzed ATP synthesis either driven by NADH oxidation or by artificial driving forces in inverted membrane vesicles of the recombinant cells.

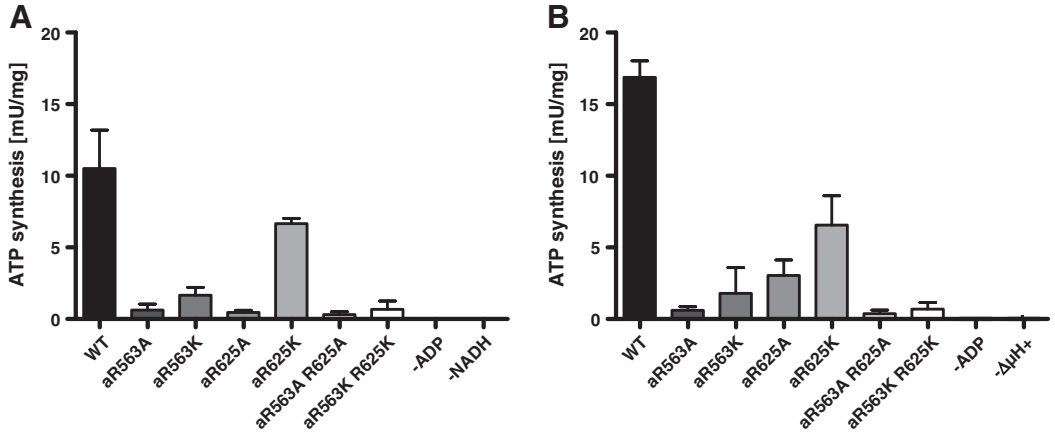

Fig. 8. Role of conserved arginine residues of subunit *a* in ATP synthesis. ATP synthesis in IMVs of *E. coli* DK8 pRIL pA43 (*a*R563A), pA47 (*a*R563K), pA48 (*a*R625A), pA49* (*a*R625K), pA50 (*a*R563A R625A) and pA51 (*a*R563K R625K) was driven either by NADH oxidation [A] or an artificial $\Delta\tilde{\mu}_{H^+}$ [B]. Vesicles containing the wild type ATP synthase were used as positive control (*E. coli* DK8 pRIL pA40hisA, WT). Negative controls (WT) contained no ADP (−ADP), no NADH (−NADH) or no $\Delta\tilde{\mu}_{H^+}$ ($-\Delta\tilde{\mu}_{H^+}$) respectively. Shown is the average of two measurements.

```
I. tartaricus       GPGVGQGYAAGKAVESVARQPEAKGDIISTMVLGQAVAESTGIYSLVIALILLYANPFVGLLG 89
A. woodii           GPGIGQGFAAGKGAEAVGRQPEAQSDIIRTMLLGAAVAETTGIYGLIVALILLFANPFF---- 82
M. mazei            ASAIAEKDIGTAAIGAMAENEGLFG---KGLIL-TVIPETIVIFGLVVALLINQ--------- 80
M. acetivorans      ASAWAEKEIGTAAIGAMAENEGLFG---KGLIL-TVIPETIVIFGLVVALLINSA-------- 82
```

Fig. 9. Sequence alignment of different *c* subunits from F_1F_O and A_1A_O ATP synthases. The conserved Na^+ binding motif (Q/E…ET/S) is highlighted.

As proven by the controls and inhibitor studies, the observed activity was clearly due to the produced A_1A_O ATP synthase. In the case of NADH-driven ATP synthesis we saw a coupling between oxidation of NADH and production of ATP, which was "lower" than in *E. coli* but nevertheless with 1 ATP/18 H^+ in the same range (data not shown). This low coupling rate was probably due to the fact that NADH oxidation can also be catalyzed by membranes but ATP synthesis requires intact membrane vesicles. To analyze the ATP synthase with regard to possible driving forces we examined ATP synthesis driven by an artificial $\Delta\tilde{\mu}_{H^+}$, ΔpH and Δψ, respectively. Experiments with the wild type enzyme indicated that a ΔpH of 1–3 is sufficient to drive ATP synthesis whereas a Δψ alone was not able to induce ATP synthesis, which is in contrast to bacterial ATP synthases. Previous studies with the F_1F_O ATP synthase from *E. coli* and *Propionigenium modestum* showed, that a Δψ alone is sufficient to drive ATP synthesis and moreover an additional ΔpH or ΔpNa can increase the ATP synthase activity but is not enough to drive ATP synthesis solitary [17,18].

A conserved carboxylate residue (glutamate or aspartate) within the *c* subunit plays a key role in the conversion of the electrochemical energy of the ion gradient to chemical energy in terms of ATP. Although not surprising due to the high sequence conservation, we provided the first experimental evidence that glutamate *c*E65 of *M. mazei* is essential for ATP synthesis in A_1A_O ATP synthases. This is consistent with its proposed function in H^+ binding and transport. Comparable studies with the ATP synthase from *E. coli* had shown that the conserved aspartate *c*D61 is essential for proton transport and ATP synthesis and cannot be exchanged to asparagine or glycine [72].

All the information gathered here is in accordance with H^+ being a coupling ion for the A_1A_O ATP synthase from *M. mazei*: NADH oxidation led to proton export but the proton gradient drives the generation of a secondary Na^+ gradient *via* Na^+/H^+ antiporter. This secondary Na^+ gradient proved competent in driving ATP synthesis [73]. Here, indications for Na^+ being (also) used were not obtained. This is all the more astonishing since the Na^+ binding motif (Q/E…ET/S) observed in subunit *c* of Na^+ F_1F_O ATP synthases is also conserved in many archaeal ATP synthases [74], notably in *M. mazei* (Fig. 9). The 8 kDa *c* subunit of *M. mazei* with its two transmembrane helices and/or subunit *a* may have additional features that determine the ion specificity. For example, the A_1A_O ATP synthase of *Methanosarcina acetivorans*, despite the conservation of the Na^+ binding motif, translocates protons and sodium ions simultaneously [75].

Besides the essential carboxyl residue of the *c* subunit the so called stator charge within subunit *a* plays a central role during ion translocation through the membrane embedded rotor domain [50,51]. According to the current models, including two half channels build up by the oligomeric *c* ring and subunit *a*, this stator charge is crucial for the release of the translocated ion at the other side of the membrane [74,76–78]. Whereas this stator charge has been identified by mutagenesis studies in several bacterial ATP synthases such as *a*R210 in *E. coli* [79], *a*R227 in *P. modestum* [80] and *a*R169 in *Bacillus* PS3 [81], less was known for archaeal ATP synthases due to the lack of a genetic system so far. In contrast to the bacterial *a* subunits with 4–5 predicted transmembrane helices, 7 to 8 helices are predicted for the *a* subunits of A_1A_O ATP synthases [11,21], which is more comparable to V_1V_O ATPases with 8 to 9 transmembrane helices predicted [82]. Sequence alignments of subunit *a* of *M. mazei* to the V_1V_O ATPase from *S. cerevisiae* revealed two conserved arginine residues. Whereas the first arginine *a*R563 turned out to be essential, exchange to either alanine or lysine led to a total loss of activity, the second one (*a*R625) can be exchanged to lysine with retention of almost 50% of the wild type activity. But as expected, loss of the positive charge by exchange to alanine led to a total loss of activity. This is consistent with mutagenesis studies of the *a* subunit of *S. cerevisiae* that revealed the first arginine *a*R735 as stator charge to be essential and the second one *a*R799 to be important for proton transport and ATP hydrolysis [52].

Three main conclusions can be derived from our work. First, the A_1A_O ATP synthase of *M. mazei* can be driven by a ΔpH whereas a Δψ alone seems not to be sufficient as driving force. Second, the conserved glutamate residue *c*E65 is essential for ATP synthesis and third, there are two conserved arginine residues within the *a* subunit that are crucial for ATP synthesis with *a*R563 most likely being the stator charge. The exact function of these two arginines remains to be analyzed by their impact on proton transport and ATP hydrolysis. The mutagenesis system described here opens the road for a further detailed molecular analyses of archaeal A_1A_O ATP synthases.

Conflict of interest

We wish to confirm that there are no known conflicts of interest associated with this publication and there has been no significant financial support for this work that could have influenced its outcome.

Acknowledgments

We thank Dr. Gabriele Deckers-Hebestreit (Universität Osnabrück, Germany) and Prof. Robert Nakamoto (University of Virginia, USA) for their help with the ATP synthesis assays, and Dr. Verena Hess for critical reading of the manuscript. The financial support of the Deutsche Forschungsgemeinschaft *via* SFB807 is gratefully acknowledged.

References

[1] E. Hilario, J.P. Gogarten, Horizontal transfer of ATPase genes — the tree of life becomes a net of life, Biosystems 31 (1993) 111–119.
[2] Y. Mukohata, K. Ihara, Situation of archaebacterial ATPase among ion-translocating ATPase, in: C.H. Kim, T. Ozawa (Eds.), Bioenergetics, Plenum Press, New York, 1990, pp. 205–216.
[3] V. Müller, G. Grüber, ATP synthases: structure, function and evolution of unique energy converters, Cell. Mol. Life Sci. 60 (2003) 474–494.
[4] R.L. Cross, V. Müller, The evolution of A-, F-, and V-type ATP synthases and ATPases: reversals in function and changes in the H^+/ATP stoichiometry, FEBS Lett. 576 (2004) 1–4.
[5] G. Grüber, M.S. Manimekalai, F. Mayer, V. Müller, ATP synthases from archaea: the beauty of a molecular motor, Biochim. Biophys. Acta 1837 (2014) 940–952.
[6] J.P. Abrahams, A.G.W. Leslie, R. Lutter, J.E. Walker, Structure at 2.8 Å resolution of F_1-ATPase from bovine heart mitochondria, Nature 370 (1994) 621–628.
[7] E.J. Boekema, B. Bottcher, The structure of ATP synthase from chloroplasts — conformational changes of CF_1 studied by electron microscopy, Biochim. Biophys. Acta 1098 (1992) 131–143.
[8] R.A. Capaldi, R. Aggeler, E.P. Gogol, S. Wilkens, Structure of the *Escherichia coli* ATP synthase and role of the gamma subunit and epsilon subunit in coupling catalytic site and proton channeling functions, J. Bioenerg. Biomembr. 24 (1992) 435–439.
[9] N. Ishii, H. Yoshimura, K. Nagayama, Y. Kagawa, M. Yoshida, 3-Dimensional structure of F_1-ATPase of thermophilic bacterium PS3 obtained by electron crystallography, J. Biochem. 113 (1993) 245–250.
[10] A. Lingl, H. Huber, K.O. Stetter, F. Mayer, J. Kellermann, V. Müller, Isolation of a complete A_1A_O ATP synthase comprising nine subunits from the hyperthermophile *Methanococcus jannaschii*, Extremophiles 7 (2003) 249–257.
[11] J. Vonck, K.Y. Pisa, N. Morgner, B. Brutschy, V. Müller, Three-dimensional structure of A_1A_O ATP synthase from the hyperthermophilic archaeon *Pyrococcus furiosus* by electron microscopy, J. Biol. Chem. 284 (2009) 10110–10119.
[12] R.A. Oot, S. Wilkens, Subunit interactions at the V_1–V_o interface in yeast vacuolar ATPase, J. Biol. Chem. 287 (2012) 13396–13406.
[13] O. Esteban, R.A. Bernal, M. Donohoe, H. Videler, M. Sharon, C.V. Robinson, D. Stock, Stoichiometry and localization of the stator subunits E and G in *Thermus thermophilus* H^+-ATPase/synthase, J. Biol. Chem. 283 (2008) 2595–2603.
[14] W.C. Lau, J.L. Rubinstein, Subnanometre-resolution structure of the intact *Thermus thermophilus* H^+-driven ATP synthase, Nature 481 (2012) 214–218.

[15] Ü. Coskun, M. Radermacher, V. Müller, T. Ruiz, G. Grüber, Three-dimensional organization of the archaeal A_1-ATPase from *Methanosarcina mazei* Gö1, J. Biol. Chem. 279 (2004) 22759–22764.

[16] G. Grüber, D.I. Svergun, Ü. Coskun, T. Lemker, M.H. Koch, H. Schägger, V. Müller, Structural insights into the A_1 ATPase from the archaeon *Methanosarcina mazei* Gö1, Biochemistry 40 (2001) 1890–1896.

[17] G. Kaim, P. Dimroth, Voltage-generated torque drives the motor of the ATP synthase, EMBO J. 17 (1998) 5887–5895.

[18] G. Kaim, P. Dimroth, ATP synthesis by F-type ATP synthase is obligatorily dependent on the transmembrane voltage, EMBO J. 18 (1999) 4118–4127.

[19] D. Stock, A.G. Leslie, J.E. Walker, Molecular architecture of the rotary motor in ATP synthase, Science 286 (1999) 1700–1705.

[20] A.M. Balakrishna, C. Hunke, G. Grüber, The structure of subunit E of the *Pyrococcus horikoshii* OT3 A-ATP synthase gives insight into the elasticity of the peripheral stalk, J. Mol. Biol. 420 (2012) 155–163.

[21] V. Müller, C. Ruppert, T. Lemker, Structure and function of the A_1A_O ATPases from methanogenic archaea, J. Bioenerg. Biomembr. 31 (1999) 15–28.

[22] E. Hilario, J.P. Gogarten, The prokaryote-to-eucaryote transition reflected in the evolution of the V/F/A-ATPase catalytic and proteolipid subunits, J. Mol. Evol. 46 (1998) 703–715.

[23] Ü. Coskun, Y.L. Chaban, A. Lingl, V. Müller, W. Keegstra, E.J. Boekema, G. Grüber, Structure and subunit arrangement of the A-type ATP synthase complex from the archaeon *Methanococcus jannaschii* visualized by electron microscopy, J. Biol. Chem. 279 (2004) 38644–38648.

[24] D.G. McMillan, S.A. Ferguson, D. Dey, K. Schroder, H.L. Aung, V. Carbone, G.T. Attwood, R.S. Ronimus, T. Meier, P.H. Janssen, G.M. Cook, A_1A_O-ATP synthase of *Methanobrevibacter ruminantium* couples sodium ions for ATP synthesis under physiological conditions, J. Biol. Chem. 286 (2011) 39882–39892.

[25] A. Kumar, M.S. Manimekalai, A.M. Balakrishna, J. Jeyakanthan, G. Grüber, Nucleotide binding states of subunit A of the A-ATP synthase and the implication of P-loop switch in evolution, J. Mol. Biol. 396 (2010) 301–320.

[26] I.B. Schäfer, S.M. Bailer, M.G. Düser, M. Börsch, R.A. Bernal, D. Stock, G. Grüber, Crystal structure of the archaeal A_1A_O ATP synthase subunit B from *Methanosarcina mazei* Gö1: implications of nucleotide-binding differences in the major A_1A_O subunits A and B, J. Mol. Biol. 358 (2006) 725–740.

[27] M. Iwata, H. Imamura, E. Stambouli, C. Ikeda, M. Tamakoshi, K. Nagata, H. Makyio, B. Hankamer, J. Barber, M. Yoshida, K. Yokoyama, S. Iwata, Crystal structure of a central stalk subunit C and reversible association/dissociation of vacuole-type ATPase, Proc. Natl. Acad. Sci. U. S. A. 101 (2004) 59–64.

[28] S. Saijo, S. Arai, K.M. Hossain, I. Yamato, K. Suzuki, Y. Kakinuma, Y. Ishizuka-Katsura, N. Ohsawa, T. Terada, M. Shirouzu, S. Yokoyama, S. Iwata, T. Murata, Crystal structure of the central axis DF complex of the prokaryotic V-ATPase, Proc. Natl. Acad. Sci. U. S. A. 108 (2011) 19955–19960.

[29] A.M. Balakrishna, C. Hunke, G. Grüber, Purification and crystallization of the entire recombinant subunit E of the energy producer A_1A_O ATP synthase, Acta Crystallogr. Sect. F: Struct. Biol. Cryst. Commun. 66 (2010) 324–326.

[30] L.K. Lee, A.G. Stewart, M. Donohoe, R.A. Bernal, D. Stock, The structure of the peripheral stalk of *Thermus thermophilus* H^+-ATPase/synthase, Nat. Struct. Mol. Biol. 17 (2010) 373–378.

[31] T. Murata, I. Yamato, Y. Kakinuma, A.G. Leslie, J.E. Walker, Structure of the rotor of the V-type Na^+-ATPase from *Enterococcus hirae*, Science 308 (2005) 654–659.

[32] S. Srinivasan, N.K. Vyas, M.L. Baker, F.A. Quiocho, Crystal structure of the cytoplasmic N-terminal domain of subunit I, a homolog of subunit *a*, of V-ATPase, J. Mol. Biol. 412 (2011) 14–21.

[33] T. Lemker, C. Ruppert, H. Stöger, S. Wimmers, V. Müller, Overproduction of a functional A_1 ATPase from the archaeon *Methanosarcina mazei* Gö1 in *Escherichia coli*, Eur. J. Biochem. 268 (2001) 3744–3750.

[34] T. Lemker, G. Grüber, R. Schmid, V. Müller, Defined subcomplexes of the A_1 ATPase from the archaeon *Methanosarcina mazei* Gö1: biochemical properties and redox regulation, FEBS Lett. 544 (2003) 206–209.

[35] Ü. Coskun, G. Grüber, M.H. Koch, J. Godovac-Zimmermann, T. Lemker, V. Müller, Cross-talk in the A_1-ATPase from *Methanosarcina mazei* Gö1 due to nucleotide-binding, J. Biol. Chem. 277 (2002) 17327–17333.

[36] G.L. Lipscomb, K. Stirrett, G.J. Schut, F. Yang, F.E. Jenney Jr., R.A. Scott, M.W. Adams, J. Westpheling, Natural competence in the hyperthermophilic archaeon *Pyrococcus furiosus* facilitates genetic manipulation: construction of markerless deletions of genes encoding the two cytoplasmic hydrogenases, Appl. Environ. Microbiol. 77 (2011) 2232–2238.

[37] H. Hippe, D. Caspari, K. Fiebig, G. Gottschalk, Utilization of trimethylamine and other N-methyl compounds for growth and methane formation by *Methanosarcina barkeri*, Proc. Natl. Acad. Sci. U. S. A. 76 (1979) 494–498.

[38] K.Y. Pisa, C. Weidner, H. Maischak, H. Kavermann, V. Müller, The coupling ion in methanoarchaeal ATP synthases: H^+ versus Na^+ in the A_1A_O ATP synthase from the archaeon *Methanosarcina mazei* Gö1, FEMS Microbiol. Lett. 277 (2007) 56–63.

[39] D.J. Klionsky, S.A. William, A. Brusilow, R.D. Simoni, *In vivo* evidence for the role of the ε subunit as an inhibitor of the proton-translocating ATPase of *Escherichia coli*, J. Bacteriol. 160 (1984) 1055–1060.

[40] D. Hanahan, Studies on transformation of *Escherichia coli* with plasmids, J. Mol. Biol. 166 (1983) 557–580.

[41] R.P. Gunsalus, W.S. Brusilow, R.D. Simoni, Gene order and gene-polypeptide relationships of the proton-translocating ATPase operon (*unc*) of *Escherichia coli*, Proc. Natl. Acad. Sci. U. S. A. 79 (1982) 320–324.

[42] S. Tanaka, S.A. Lerner, E.C.C. Lin, Replacement of a phosphoenolpyruvate-dependent phosphotransferase by a nicotinamide adenine dinucleotide-linked dehydrogenase for the utilization of mannitol, J. Bacteriol. 93 (1967) 642–648.

[43] M.M. Bradford, A rapid and sensitive method for the quantification of microgram quantities of protein utilizing the principle of proteine-dye-binding, Anal. Biochem. 72 (1976) 248–254.

[44] H. Towbin, T. Staehelin, J. Gordon, Electrophoretic transfer of proteins from polyacrylamide gels to nitrocellulose sheets: procedure and some applications, Proc. Natl. Acad. Sci. U. S. A. 76 (1979) 4350–4354.

[45] G.A. Kimmich, J. Randles, J.S. Brand, Assay of picomole amounts of ATP, ADP and AMP using the luciferase enzyme system, Anal. Biochem. 69 (1975) 187–206.

[46] M.J. Maher, S. Akimoto, M. Iwata, K. Nagata, Y. Hori, M. Yoshida, S. Yokoyama, S. Iwata, K. Yokoyama, Crystal structure of A_3B_3 complex of V-ATPase from *Thermus thermophilus*, EMBO J. 28 (2009) 3771–3779.

[47] F.S. Esch, P. Bohlen, A.S. Otsuka, M. Yoshida, W.S. Allison, Inactivation of the bovine mitochondrial F1-ATPase with dicyclohexyl[14C]carbodiimide leads to the modification of a specific glutamic acid residue in the beta subunit, J. Biol. Chem. 256 (1981) 9084–9089.

[48] M.W. McEnery, P.L. Pedersen, Diethylstilbestrol, a novel type of F_O-directed probe of the mitochondrial proton ATPase, J. Biol. Chem. 261 (1986) 1745–1752.

[49] C. Ruppert, S. Wimmers, T. Lemker, V. Müller, The A_1A_O ATPase from *Methanosarcina mazei*: cloning of the 5′ end of the *aha* operon encoding the membrane domain and expression of the proteolipid in a membrane-bound form in *Escherichia coli*, J. Bacteriol. 180 (1998) 3448–3452.

[50] G. Deckers-Hebestreit, K. Altendorf, The F_OF_1-type ATP synthases of bacteria: structure and function of the F_O complex, Annu. Rev. Microbiol. 50 (1996) 791–824.

[51] R.H. Fillingame, H^+ transport and coupling by the F_O sector of the ATP synthase — insights into the molecular mechanism of function, J. Bioenerg. Biomembr. 24 (1992) 485–491.

[52] S. Kawasaki-Nishi, T. Nishi, M. Forgac, Arg-735 of the 100 kDa subunit *a* of the yeast V-ATPase is essential for proton translocation, Proc. Natl. Acad. Sci. U. S. A. 98 (2001) 12397–12402.

[53] K.Y. Pisa, H. Huber, M. Thomm, V. Müller, A sodium ion-dependent A_1A_O ATP synthase from the hyperthermophilic archaeon *Pyrococcus furiosus*, FEBS J. 274 (2007) 3928–3938.

[54] W.C. Lau, J.L. Rubinstein, Structure of intact *Thermus thermophilus* V-ATPase by cryo-EM reveals organization of the membrane-bound V_O motor, Proc. Natl. Acad. Sci. U. S. A. 107 (2010) 1367–1372.

[55] S. Peinemann, R. Hedderich, M. Blaut, R.K. Thauer, G. Gottschalk, ATP synthesis coupled to electron transfer from H_2 to the heterodisulfide of 2-mercaptoethanesulfonate and 7-mercaptoheptanoylthreonine phosphate in vesicle preparations of the methanogenic bacterium strain Gö1, FEBS Lett. 263 (1990) 57–60.

[56] S. Bäumer, T. Ide, C. Jacobi, A. Johann, G. Gottschalk, U. Deppenmeier, The $F_{420}H_2$ dehydrogenase from *Methanosarcina mazei* is a redox-driven proton pump closely related to NADH dehydrogenases, J. Biol. Chem. 275 (2000) 17968–17973.

[57] U. Deppenmeier, M. Blaut, G. Gottschalk, H_2:heterodisulfide oxidoreductase, a second energy-conserving system in the methanogenic strain Gö1, Arch. Microbiol. 155 (1991) 272–277.

[58] S.P. Tsunoda, R. Aggeler, H. Noji, K. Kinosita Jr., M. Yoshida, R.A. Capaldi, Observations of rotation within the F_OF_1-ATP synthase: deciding between rotation of the F_o *c* subunit ring and artifact, FEBS Lett. 470 (2000) 244–248.

[59] C. Etzold, G. Deckers-Hebestreit, K. Altendorf, Turnover number of *Escherichia coli* F_OF_1 ATP synthase for ATP synthesis in membrane vesicles, Eur. J. Biochem. 243 (1997) 336–343.

[60] K.I. Inatomi, Characterization and purification of the membrane-bound ATPase of the archaebacterium *Methanosarcina barkeri*, J. Bacteriol. 167 (1986) 837–841.

[61] M. Lübben, H. Lunsdorf, G. Schäfer, The plasma membrane ATPase of the thermoacidophilic archaebacterium *Sulfolobus acidocaldarius*. Purification and immunological relationships to F_1-ATPases, Eur. J. Biochem. 167 (1987) 211–219.

[62] M. Lübben, G. Schäfer, Chemiosmotic energy conservation of the thermoacidophile Sulfolobus acidocaldarius: oxidative phosphorylation and the presence of an FO-related N′, N′-dicyclohexylcarbodiimide-binding proteolipid, J. Bacteriol. 171 (1989) 6106–6116.

[63] L.I. Hochstein, H. Kristjansson, W. Altekar, The purification and subunit structure of a membrane-bound ATPase from the archaebacterium *Halobacterium saccharovorum*, Biochem. Biophys. Res. Commun. 147 (1987) 295–300.

[64] T. Nanba, Y. Mukohata, A membrane-bound ATPase from *Halobacterium halobium*: purification and characterization, J. Biochem. 102 (1987) 591–598.

[65] E. Scheel, G. Schäfer, Chemiosmotic energy conservation and the membrane ATPase of *Methanolobus tindarius*, Eur. J. Biochem. 187 (1990) 727–735.

[66] L.I. Hochstein, H. Stanlotter, Purification and properties of an ATPase from *Sulfolobus solfataricus*, Arch. Biochem. Biophys. 295 (1992) 153–160.

[67] K.I. Inatomi, Y. Kamagata, K. Nakamura, Membrane ATPase from the aceticlastic methanogen *Methanothrix thermophila*, J. Bacteriol. 175 (1993) 80–84.

[68] W. Chen, J. Konisky, Characterization of a membrane-associated ATPase from *Methanococcus voltae*, a methanogenic member of the archaea, J. Bacteriol. 175 (1993) 5677–5682.

[69] K. Steinert, S. Bickel-Sandkötter, Isolation, characterization, and substrate specificity of the plasma membrane ATPase of the halophilic archaeon *Haloferax volcanii*, Z. Naturforsch. 51 (1996) 29–39.

[70] K. Ihara, S. Watanabe, K. Sugimura, Y. Mukohata, Identification of proteolipid from an extremely halophilic archaeon *Halobacterium salinarum* as an N′, N′-dicyclohexyl-carbodiimide binding subunit of ATP synthase, Arch. Biochem. Biophys. 341 (1997) 267–272.

[71] R. Wilms, C. Freiberg, E. Wegerle, I. Meier, F. Mayer, V. Müller, Subunit structure and organization of the genes of the A_1A_O ATPase from the archaeon *Methanosarcina mazei* Gö1, J. Biol. Chem. 271 (1996) 18843–18852.

[72] J. Hoppe, H.U. Schairer, P. Friedl, W. Sebald, An Asp-Asn substitution in the proteolipid subunit of the ATP-synthase from *Escherichia coli* leads to a non-functional proton channel, FEBS Lett. 145 (1982) 21–29.
[73] W. Laubinger, G. Deckers-Hebestreit, K. Altendorf, P. Dimroth, A hybrid adenosinetriphosphatase composed of F_1 of *Escherichia coli* and F_O of *Propionigenium modestum* is a functional sodium ion pump, Biochemistry 29 (1990) 5458–5463.
[74] F. Mayer, V. Müller, Adaptations of anaerobic archaea to life under extreme energy limitation, FEMS Microbiol. Rev. 38 (2013) 449–472.
[75] K. Schlegel, V. Leone, J.D. Faraldo-Gomez, V. Müller, Promiscuous archaeal ATP synthase concurrently coupled to Na^+ and H^+ translocation, Proc. Natl. Acad. Sci. U. S. A. 109 (2012) 947–952.
[76] S.B. Vik, B.J. Antonio, A mechanism of proton translocation by F_1F_O ATP synthases suggested by double mutants of the *a* subunit, J. Biol. Chem. 269 (1994) 30364–30369.
[77] W. Junge, H. Lill, S. Engelbrecht, ATP synthase: an electrochemical transducer with rotatory mechanics, Trends Biochem. Sci. 22 (1997) 420–423.
[78] D. Pogoryelov, O. Yildiz, J.D. Faraldo-Gómez, T. Meier, High-resolution structure of the rotor ring of a proton-dependent ATP synthase, Nat. Struct. Mol. Biol. 16 (2009) 1068–1073.
[79] B.D. Cain, R.D. Simoni, Proton translocation by the F_1F_0 ATPase of *Escherichia coli*. Mutagenic analysis of the *a* subunit, J. Biol. Chem. 264 (1989) 3292–3300.
[80] F. Wehrle, Y. Appoldt, G. Kaim, P. Dimroth, Reconstitution of F_O of the sodium ion translocating ATP synthase of *Propionigenium modestum* from its heterologously expressed and purified subunits, Eur. J. Biochem. 269 (2002) 2567–2573.
[81] N. Mitome, S. Ono, H. Sato, T. Suzuki, N. Sone, M. Yoshida, Essential arginine residue of the F_O-*a* subunit in F_oF_1-ATP synthase has a role to prevent the proton shortcut without *c*-ring rotation in the F_O proton channel, Biochem. J. 430 (2010) 171–177.
[82] S. Wilkens, M. Forgac, Three-dimensional structure of the vacuolar ATPase proton channel by electron microscopy, J. Biol. Chem. 276 (2001) 44064–44068.